

APPLICATION OF AN EVAPORATION DUCT CLIMATOLOGY IN THE LITTORAL

Richard A. Paulus* and Kenneth D. Anderson
Atmospheric Propagation Branch

SPAWARSYSCEN SAN DIEGO D858
49170 PROPAGATION PATH
SAN DIEGO CA 92152-7385

Ph: 619-553-1424 Fax: 619-553-1417
E-mail: paulus@spawar.navy.mil

Ph: 619-553-1420 Fax: 619-553-1417
E-mail: kenn@spawar.navy.mil

Sponsored by the Office of Naval Research (ONR-322MM)

Introduction

The refractive structure of the marine atmospheric surface layer at microwave frequencies can be characterized by a parameter called the “evaporation duct height”, the height of the minimum in the profile of modified refractivity. Profiles of meteorological variables in the surface layer can be calculated with well-known flux profile relationships using bulk measurements of air temperature, relative humidity, wind speed, and sea surface temperature (Fig. 1). A data base of these measurements from ocean weather stations and ships of opportunity is maintained by the National Climatic Data Center Asheville and a set of data with a period of record generally from 1970 to 1984 was used to construct an evaporation duct climatology [Anderson, 1987]. This climatology has been used successfully to statistically model evaporation duct propagation [Hitney and Vieth, 1990] and frequency diversity effects [Hitney and Hitney, 1990]. The sites for these two studies were the Aegean Sea and the North Sea, predominately under open ocean influence.

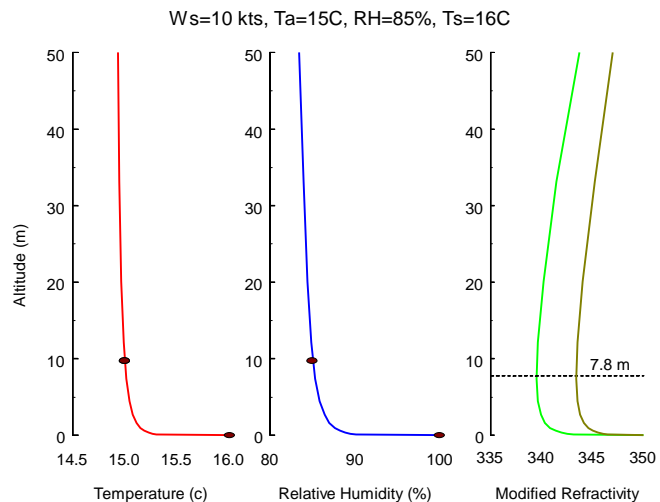


Figure 1. Example surface layer profiles of temperature, relative humidity, and modified refractivity for the bulk parameters measured at 10 m and the sea surface as indicated by the dots. The calculated evaporation duct height is 7.8 m on the light green profile. The brown profile is a 7.8 m neutral evaporation duct neglecting the effects of stability.

In our paper, this evaporation duct climatology is used to predict propagation loss on both a monthly and annual basis in coastal regions strongly under continental influence. Distributions of multifrequency propagation loss data on a slightly over-the-horizon path off the coast of Lorient, France [Christophe et al., 1995] are compared to climatological predictions. The prevailing winds near Lorient have a westerly component, providing a predominantly open ocean influence over the propagation path. However, offshore easterly winds are relatively common. Distributions of long term propagation loss data for 2 near-horizon propagation links off the coast of Wallops Island, VA [Goldhirsh et al., 1994] are compared to annual climatological predictions. The Wallops Island offshore area is under a prevailing westerly (offshore) wind and the influence of the Gulf Stream and Labrador currents. Distributions of propagation loss for a much longer, over-the-horizon propagation link between Wallops Island and Dam Neck, VA [Goldhirsh and Musiani, 1999] are also compared with climatological predictions. The mid-Atlantic offshore area is similarly under a prevailing offshore wind and the Gulf Stream and Labrador current influences.

Climatological Propagation for the Lorient Coastal Area

NATO/AC243/Panel3/RSG8(PSG) [Christophe et al., 1995] reviews a multifrequency propagation experiment conducted in 1989 on a 27.7 km over-the-horizon path offshore of

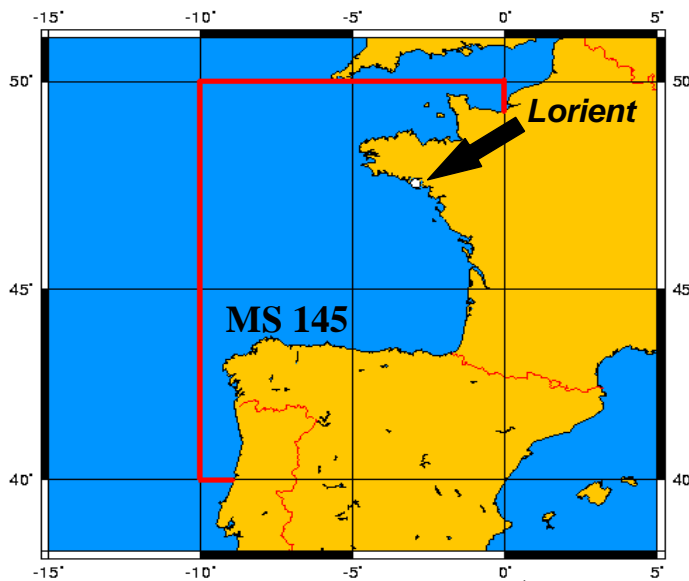


Figure 2. The Lorient offshore area is in Marsden square 145, bounded in red (40N to 50N and the Prime Meridian to 10W).

Lorient, France. The experiment was conducted between mid-September and mid-December. The evaporation duct climatology is organized by Marsden squares (MS), 10° latitude by 10° longitude geographic areas. The Lorient offshore area is in MS 145 (Figure 2). This area is under the influence of a prevailing westerly (onshore) flow but is also routinely affected by easterly winds off the European continent. Meteorological data collected during the experiment showed the air to be warmer than the water approximately 75% of the time indicating a pronounced continental influence [Rogers and Paulus, 1996]. The annual distribution of evaporation duct height is shown in Figure 3; the mean evaporation duct height is 7.8 m.

For propagation model input, refractivity profiles can be generated parametrically in duct height using

$$M(z) = M_0 + 0.13z - 0.13d \ln \left(\frac{z + z_0}{z_0} \right) \quad (1)$$

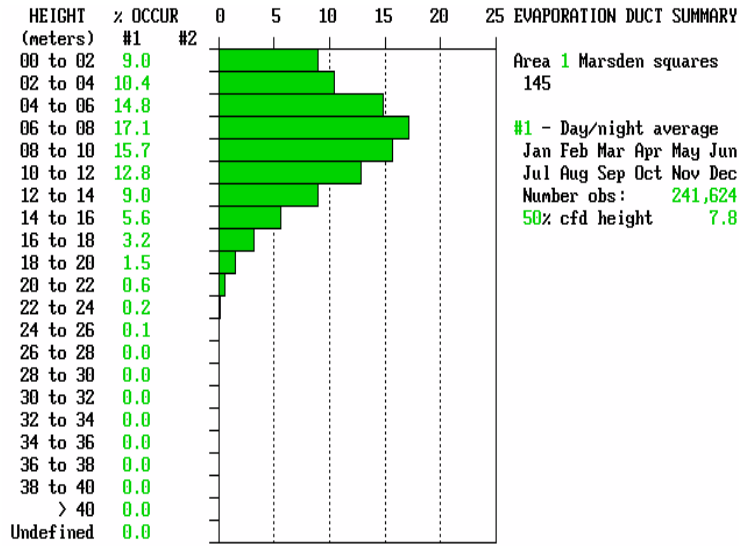


Figure 3. Annual distribution of evaporation duct height for Marsden square 145.

where M is modified refractivity, z is altitude in m, M_0 is the value of modified refractivity at the sea surface, d is evaporation duct height in m, and z_0 is the aerodynamic roughness parameter (set to 1.5×10^{-4} m here). Equation (1) assumes thermally neutral conditions and thus does not account for stability effects on the shape of the profile. A neutral profile is shown as the brown curve in Figure (1) which is nearly the same shape as the green profile except for the difference in gradient in the very lowest levels of the profiles. For common departures from neutrality,

propagation calculations have shown that a neutral profile is a reasonable approximation, provided that the duct height is determined from observed meteorology [Anderson, 1990]. We modeled the expected distribution of signal level using the MLAYER waveguide propagation model [Baumgartner et al., 1983], the link geometry, and the distributions of evaporation duct heights. Using MLAYER, propagation loss values were generated for each frequency for evaporation duct heights from 0 to 20 m and these were weighted by the percent occurrence of the evaporation duct height. The results for 3, 5.6, 10.5, and 16 GHz are shown in Figures 4 through 7 respectively. There is excellent agreement between the modeled and observed distributions. Figure 4 shows that the 3.0 GHz signals were enhanced by about 7 dB above the

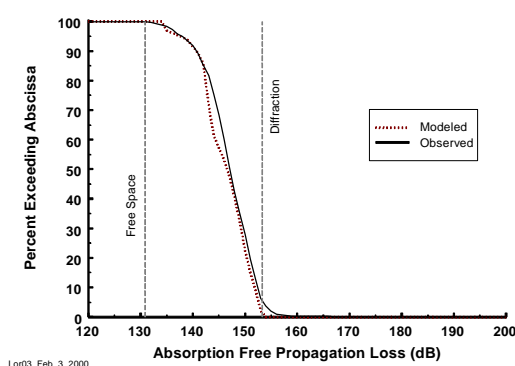


Figure 4. Distribution of observed (solid black line) and modeled (dotted red line) propagation loss at 3 GHz. Free space and diffraction levels are indicated by vertical dashed lines.

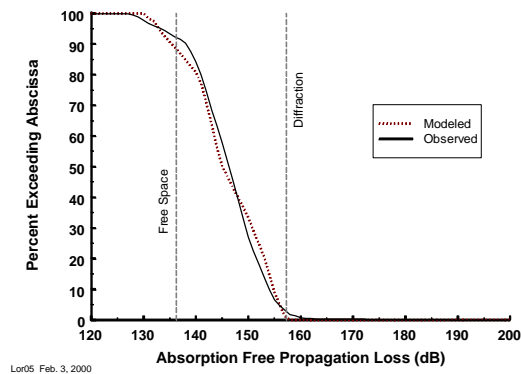


Figure 5. Distribution of observed (solid black line) and modeled (dotted red line) propagation loss at 5.6 GHz. Free space and diffraction levels are indicated by vertical dashed lines.

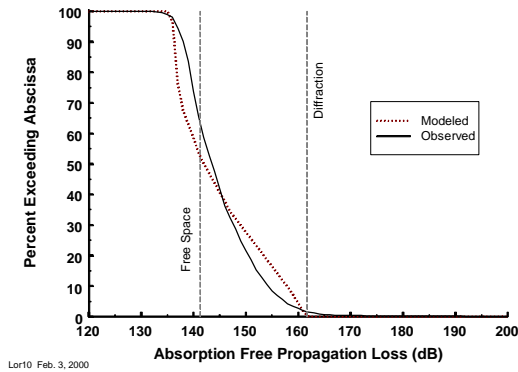


Figure 6. Distribution of observed (solid black line) and modeled (dotted red line) propagation loss at 10 GHz. Free space and diffraction levels are indicated by vertical dashed lines.

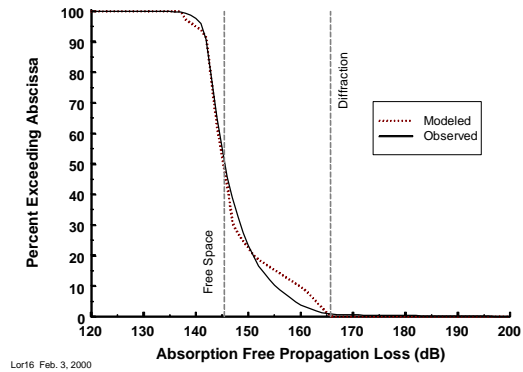


Figure 7. Distribution of observed (solid black line) and modeled (dotted red line) propagation loss at 16 GHz. Free space and diffraction levels are indicated by vertical dashed lines.

standard atmosphere diffraction level at the median; Figure 5 shows that 5.6 GHz signals were enhanced by about 10 dB; Figure 6 shows that the 10.5 GHz signals were enhanced about 18 dB; and Figure 7 shows that the 16 GHz signals were enhanced about 20 dB to the free space level. These results indicate that the evaporation duct was the dominant propagation mechanism and the climatology is capable of representing expected signal distributions on a monthly time scale in this littoral area.

Climatological Propagation for the Wallops Island Coastal Area

Goldhirsh *et al.* [1994] reported three years of fade statistics for two line-of-sight propagation links operating at 4.7 GHz off the coast of Wallops Island, VA. The transmitter was located on Parramore Island and receivers were located on Assateague Island on a tower and a lighthouse. The tower link was 39 km long (0.97 times horizon range for the 36.9 m transmitter and 13.7 m receiver) and the lighthouse link was 44.1 km long (0.83 times horizon range for the 45.5 m receiver). We modeled the expected distributions of signal levels on these two links using the Radio Physical Optics (RPO) propagation model [Hitney, 1992], the link geometry, and distributions of evaporation duct heights for ocean areas off the mid-Atlantic coast.

The Wallops Island offshore area is in Marsden square 116 (Figure 8). This area is not only under the influence of a prevailing westerly (offshore) flow but is also influenced by the presence of the Gulf Stream cutting across the southeastern half of this square. In opposition to the Gulf Stream is the Labrador current flowing southerly along the coast. These currents cause markedly different sea surface temperatures (SST) across MS 116. An example SST analysis is shown in Figure 9. Based on SST, it appears that the offshore Wallops Island area is better represented by MS 151 to the northeast than MS 116. Because of the complexity resulting from these currents, we utilized evaporation duct distributions for both Marsden squares 116 and 151 in our analysis. These are shown in Figure 10. The distributions are distinctly different with a mean duct height

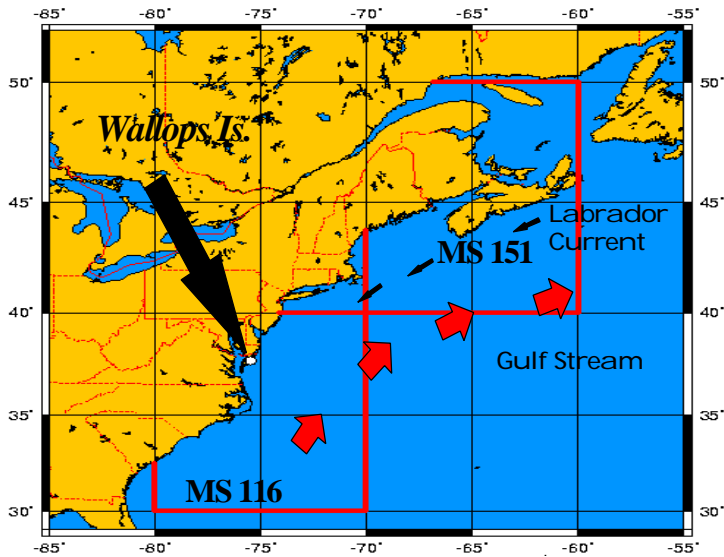


Figure 8. Marsden squares 116 and 151 along the east coast of North America with symbols for the general location and flow of the Gulf Stream and Labrador Current.

climatological distributions do bound the data at the median and over the middle part of the distribution with the MS 151 distribution being more representative. The differences between the distributions at the higher signal levels are due in part to surface-based ducts that occur about 14% of the time (based on historical radiosonde ducting statistics [Ortenburger, 1979]). The

of 14.4 m in MS 116 and 5.1 m in MS 151. Using RPO, propagation loss values were generated for each link for evaporation duct heights from 0 to 36 m in 2 meter increments and these were weighted by the percent occurrence of the evaporation duct height. We expected that these distributions would bound Goldhirsh's data. These results are shown in Figures 11 and 12. Figure 11 shows good agreement between Goldhirsh's data and the climatological distributions. This is expected because the lighthouse link was well within the horizon and the difference between free space and diffraction is only 3 dB. Figure 12 shows that the two

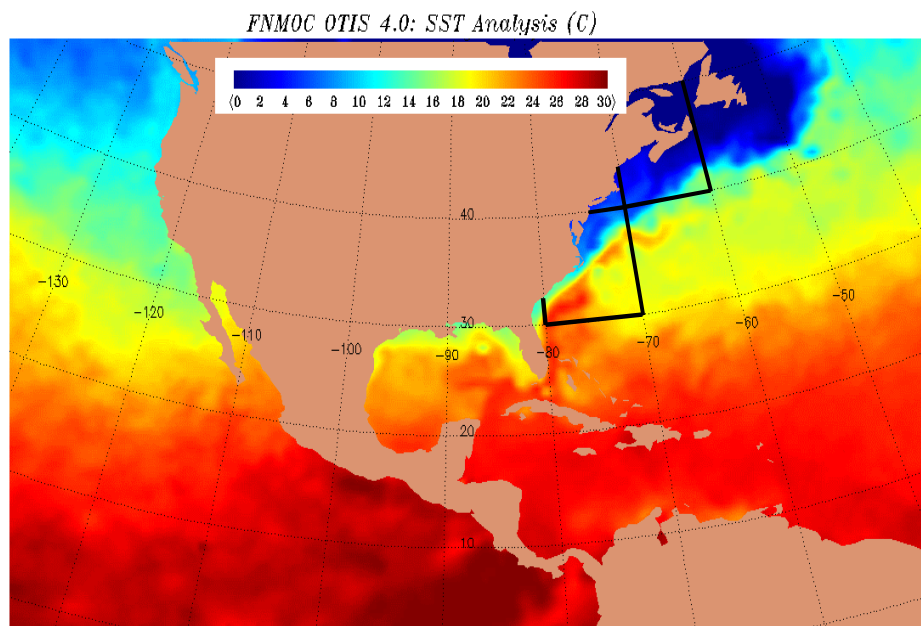


Figure 9. An example sea surface temperature analysis from the Fleet Numerical Meteorology and Oceanography Center.

differences between the distributions at the lower signal levels are due to subrefraction which is reported to occur about 10% of the time [Goldhirsh et al., 1994].

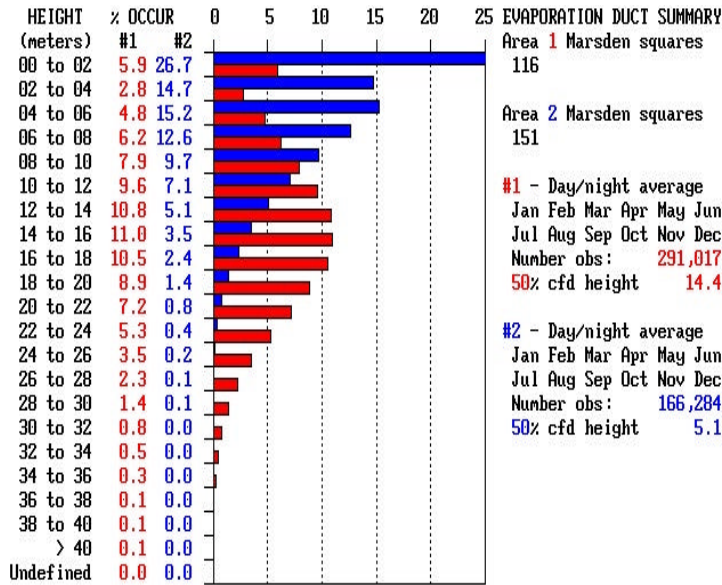


Figure 10. Annual distribution of evaporation duct height for Marsden squares 116 (red) and 151 (blue).

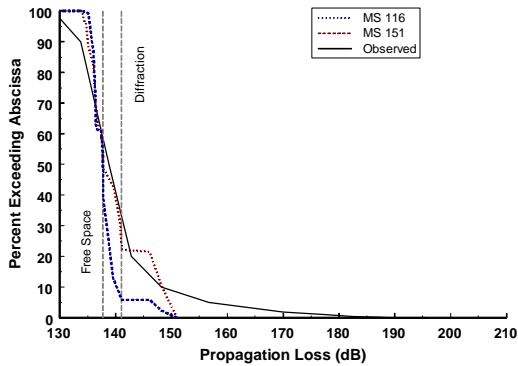


Figure 11. Distributions of data (black), MS 116 (blue), and MS151(red) for the lighthouse link. The free space and diffraction propagation loss values are 139 and 141 dB.

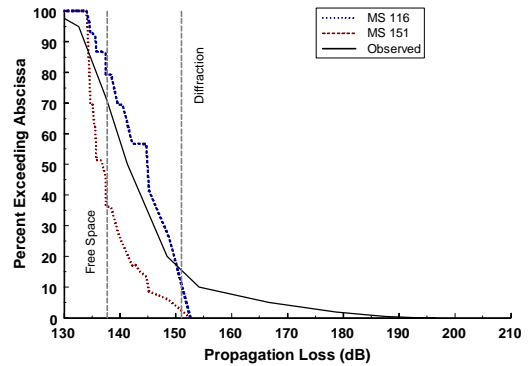


Figure 12. Distributions of data (black), MS 116 (blue), and MS151(red) for the lookout tower link. The free space and diffraction propagation loss values are 138 and 151 dB.

Climatological Propagation for the Wallops Island to Dam Neck Coastal Area

Goldhirsh and Musiani [1999] reported one year of statistics for a 128 km over-the-horizon C-band propagation link between Dam Neck and Wallops Island, VA. The transmitter at Dam Neck was at 53.6 m and the receiver at Wallops Island was at 43.4 m making this path about 2.2

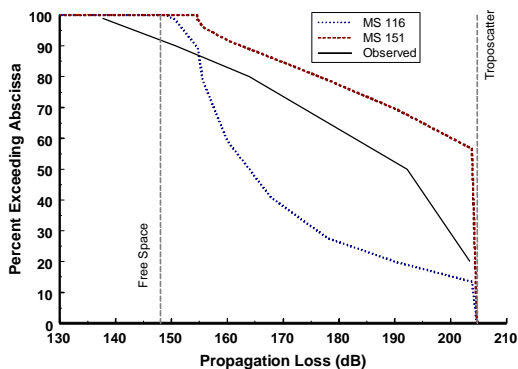


Figure 13. Distributions of data (black), MS 116 (blue), and MS151(red) for the Dam Neck to Wallops Island link. The free space and troposcatter propagation loss values are 148 and 205 dB.

times horizon range. Similar to the analysis above, propagation loss values were generated for this link for evaporation duct heights from 0 to 36 m in 2 meter increments and these results were weighted by the percent occurrence of the evaporation duct height in each of the two Marsden squares. The results are shown in Figure 13. Again, the climatological distributions bound the measured data at and around the median. However, the spread between the 2 climatological distributions at the median is 40 dB and does not provide much useful information to a user. The effects of surface-based ducts are the likely cause of the high signal levels (up to and above free space) in the measured data.

Limitations of the Evaporation Duct Climatology

In the case of Lorient and Marsden square 145, the annual evaporation duct height distribution averaged over the entire square gave excellent results. In the case of Wallops Island and Marsden square 116, it was necessary to recognize that the Gulf Stream and its annual meander would impact sea surface temperature. Thus the evaporation duct height distribution averaged over the entire square would not be representative of the Wallops site. Using statistics from a neighboring square allowed us to closely bound the data for the near-horizon propagation links. However, for the twice horizon-range propagation link, the spread of climatological predictions was too wide to closely bound the data. Thus, averaging over a region as large as a Marsden square is not effective for long, over-the horizon paths if there is a marked variation of climatic parameters across the region. Another, perhaps better, approach is to compile statistics over sub-squares where sufficient observations are available.

Two refractive phenomena are not fully accounted for in the evaporation duct climatology: subrefraction and surface-based ducts. In the Wallops Island data, subrefraction has an impact about 10% of the time. This could possibly be included by using what Jeske [1973] referred to as an “anti-duct”, a situation in which a negative evaporation duct height is calculated. Using a negative d in Equation 1 results in a subrefractive profile. It has not been demonstrated that using negative duct heights produces representative results.

Statistics of surface-based ducting derived from radiosondes launched at sea are very sparse. Coastal and island statistics may be used with caution, recognizing the problem that overland soundings may not be representative of refractive conditions downwind over the water. Furthermore, only the percent occurrence of surface-based ducting is available such that only a

qualitative statement can be made about signal levels associated with this propagation mechanism.

Conclusion

The evaporation duct climatology can be used to predict median signal level for surface-to-surface propagation, even in coastal environments strongly under a coastal zone influence. Other coastal areas with marked climatological differences across a Marsden square do not have sufficient spatial resolution to represent propagation. Possible enhancements to the data base include decreasing the area over which the statistics are determined and including statistics for subrefraction in the surface layer.

Acknowledgments

This work is sponsored by Dr. Scott Sandgathe, Office of Naval Research, ONR322.

References

Anderson, K.D., "Worldwide Distributions of Shipboard Surface Meteorological Observations for EM Propagation Analysis," NOSC Technical Document 1150 (ADA188771), 40 pp., Naval Ocean Systems Center, San Diego, CA, Sep 1987.

Anderson, K.D., "94-GHz Propagation in the Evaporation Duct," *IEEE Trans. Antennas Propag.*, 38(5), pp. 746-753, May 1990.

Baumgartner, G.B., Jr., H.V. Hitney, and R.A. Pappert, "Duct Propagation Modelling for the Integrated Refractive Effects Prediction System (IREPS)," *IEE Proc. Vol. 130, Part F*, no. 7, pp. 630-642, December 1983.

Christophe, F., N. Douchin, Y. Hurtaud, D. Dion, R. Makarushka, H. Heemskerk, and K. Anderson, "Overview of NATO/AC 243/Panel 3 Activities Concerning Radiowave Propagation in Coastal Environments," in AGARD CP-567 (ADA296641), Propagation Assessment in Coastal Environments, February 1995.

Goldhirsh, J., G.D. Dockery, and B.H. Musiani, "Three years of C band signal measurements for overwater, line-of-sight links in the mid-Atlantic coast," *Radio Sci.*, 29(6), pp.1421-1431, 1994.

Goldhirsh, J and B.H. Musiani, "Signal level statistics and case studies for an over-the-horizon mid-Atlantic coastal link operating at C-band," *Radio Sci.*, 34(2), pp. 355-370, 1999.

Hitney, H.V., "Hybrid Ray Optics and Parabolic Equation Methods for Radar Propagation Modeling," *Radar 92*, IEE Conference Publication No. 365, pp. 58-61, Brighton, UK, 12-13 Oct 1992.

Hitney, H.V. and R. Vieth, "Statistical Assessment of Evaporation Duct Propagation," *IEEE Trans. Antennas Propag.*, 38(6), pp. 794-799, June 1990.

Hitney, H.V. and L.R. Hitney, "Frequency Diversity Effects of Evaporation Duct Propagation," *IEEE Trans. Antennas Propag.*, 38(10), pp. 1694-1700, October 1990.

Jeske, H., "State and Limits of Prediction Methods of Radar Wave Propagation Conditions Over Sea," in *Modern Topics in Microwave Propagation and Air-Sea Interaction*, 131-148, A. Zanca, ed., Reidel Publishers, 1973.

Ortenburger, L.N., "World-Wide Statistics of Tropospheric Ducting Characteristics," in Proceedings of Conference on Atmospheric Refractive Effects Assessment, NOSC TD 260 (ADA071781), 15 June 1979.

Rogers, L.T. and R.A. Paulus, "Measured performance of evaporation duct models," Proc. Battlespace Atmospheric Conference, BAC'96, 3-5 Dec 1996, NRaD TD 2938 (ADA323038), 1996.